Title

Temperature Tuning the Catalytic Reactivity of Cu-Doped Porous Metal Oxides with Lignin Models

Journal

ACS Sustainable Chemistry & Engineering, 6(2)

ISSN

2168-0485

Authors

Bernt, Christopher M
Manesewan, Hussaya
Chui, Megan
et al.

Publication Date

2018-02-05

DOI

10.1021/acssuschemeng.7b03969

Temperature tuning the catalytic reactivity of Cu-doped porous metal oxides with lignin models.

Christopher M. Bernt,[a] Hussaya Manesewan,[a] Megan Chui,[a] Mauricio Boscolo,[a,b] Peter C. Ford[a,*]

[a] Department of Chemistry and Biochemistry, University of California, Santa Barbara; Santa Barbara, CA, 93106-9510 USA.

[b] Depto. Quimica e Ciencias Ambientais-IBILCE, São Paulo State University-UNESP, Cristovao Colombo, 2265. São José do Rio Preto, São Paulo, Brazil.

email: PCF: ford@chem.ucsb.edu

Supporting Information Placeholder

ABSTRACT: Reported are the temperature dependencies of the temporal product evolution for lignin model compounds over copper doped porous metal oxide (CuPMO) in supercritical-methanol (sc-MeOH). These studies investigated 1-phenylethanol (PPE), benzyl phenyl ether (BPE), dihydrobenzofuran (DHBF) and phenol over operating temperature ranges from 280 to 330 °C. The first three model compounds represent the β-O-4 and α-O-4 linkages in lignin as well as the furan group commonly found in the β-5 linkage. Phenol was investigated due to its key role in product proliferation as noted in earlier studies with this Earth-abundant catalyst. In general, the apparent activation energies for ether hydrogenolysis proved to be significantly lower than that for phenol hydrogenation, a major side reaction leading to product proliferation. Thus, temperature tuning is a promising strategy to preserve product aromaticity as demonstrated by the more selective conversion of BPE and PPE at the lower temperatures. Rates of methanol reforming over CuPMO were also studied over the temperature range 280 – 320 °C, since it is this process that generates the reducing equivalents for this catalytic system. In the absence of substrate, the gaseous products H_2, CO, and CO_2 were formed in ratios stoichiometrically consistent with catalyzed methanol reformation and water gas shift reactions. The latter studies suggest that the H_2 production ceases to be rate limiting early in batch reactor experiments, but also suggest that H_2 overproduction may contribute to product proliferation.

KEYWORDS: *Lignin models, Heterogenous catalysis, Supercritical methanol, Activation Energies, Methanol reforming*

INTRODUCTION

Lignocellulose is a highly abundant and renewable source of functional carbon that is an attractive green alternative to fossil carbon resources. However, a major constituent, lignin, (15-40% of lignocellulose depending on the plant type and origin)[1,2] remains underutilized owing to its chemical complexity.[3] Despite its potential as a carbon-neutral source of aromatic chemicals, lignin is currently treated mostly as a waste product or simply burned to produce low grade heat. Successful commodification of lignin would add value to intentionally planted lignocellulosic crops and to agriculture and forest wastes.[1]

Lignin is a complex biological macromolecule that is unique among biomass components in its frequency of aromatic units and relatively high energy density. The primary barrier to lignin utilization is the efficient, and sufficiently selective, breakdown of this material into chemical feedstocks that could be used for sophisticated fuels or synthetic precursors. Much of its complexity is due to the biosynthetic routes that form lignin via radical polymerization of monolignols, which are propylphenol derivatives. The majority of the linkages between the monolignol components are aryl ethers, although there is some cross linking via carbon-carbon bonds.[4-6] Developing selective methodologies to cleave such linkages while preserving the aromatic functionality during lignin disassembly has been a major goal of our laboratory and others.[7-15]

This laboratory has focused on reductive approaches to the disassembly of lignin and lignocellulose composites using Earth-abundant catalysts. In the course of such studies, it was found that copper-doped porous metal oxides (CuPMOs) derived by calcination of copper-doped hydrotalcites (CuHTCs) are effective catalysts in supercritical methanol (sc-MeOH) for the hydrogenolysis (HDG) and hydrodeoxygenation (HDO) of these materials to organic liquids.[9,16,17] The reducing equivalents needed are generated by the concurrent catalyzed reforming of MeOH. A key feature is that these transformations occur without forming organic chars. Subsequent studies have exploited these and similar PMO supported catalysts in related lignin disassembly pathways.[7,9,11,17,18]

The efficacy of the CuPMO catalyzed lignin disassembly in sc-MeOH has led this laboratory to probe the hydrogenolysis of various aryl ether models with the goals of elucidating the relative HDG rates for characteristic lignin linkages and of identifying the intermediate species responsible for product proliferation. However, the monomeric and oligomeric fragments ini-

tially formed were found to have undergone subsequent hydrogenation (HYD) of aromatic rings as well as various methylation steps. Such information provides guidelines for defining reaction conditions that improve the selectivity and valorization of the product stream from lignin and other renewable biomass substrates. For example, these studies demonstrated that phenolic byproducts are particularly reactive toward undesirable side reactions,[10] and have explored modifications of the solvent medium[8] and of the catalyst[11] to address this issue. The present investigation further probes the temperature dependence of the catalysis rates with several model substrates. The goal was to develop deeper understanding of what parameters can be modified to control product distributions, with particular emphasis on tuning the relative rates of the HDG and HYD processes. Also described is an investigation of the temperature dependence of the methanol reforming that is an essential component of this catalytic system.

EXPERIMENTAL SECTION

Materials and syntheses. Dihydrobenzofuran, diphenyl ether, benzyl-phenyl ether and the materials listed in the synthesis of PPE were purchased from Sigma-Aldrich, Acros or TCI and were largely used as supplied. An exception was benzyl phenyl ether, which often was discolored as received. In that case, the BPE was dissolved in a dilute methanolic NaOH solution, then precipitated from this solution by the dropwise addition of water. The precipitate was filtered to afford the white powder used in these studies. 2-Phenoxy-1-phenylethan-1-ol was prepared from the reduction of 2-phenoxy-1-phenylethan-1-one which was in turn synthesized from 2-bromo-acetophenone and phenol via a procedure adapted from a published protocol.[20] See Supporting Information (SI) for details.

The catalysis used in these studies was a copper-doped porous metal oxide Cu_{20}PMO prepared by calcining a copper-doped hydrotalcite (CuHTC) precursor. The CuHTC prepared via a co-precipitation method according to procedures described by Cosimo et al.[21] and subsequently modified by Macala et al.[14] (See SI for details). The CuHTC is a 3:1 Mg^{2+} : Al^{3+} double layer hydrotalcite in which 20% of the dipositive Mg^{2+} has been replaced in the synthesis by Cu^{2+}. The Cu_{20}PMO for each catalysis experiment was freshly prepared by calcining the CuHTC overnight (for at least 12 h) at 460 °C.

Reaction Procedures. Catalysis runs were all carried out in duplicate (at a minimum) for each time-point, temperature and substrate. Stock solutions for reactions with lignin models were prepared with 1 mmol of substrate and 20 µL of n-decane (as an internal standard) per 3.0 mL of methanol. A typical preparation would consist of 20 mL of stock solution to provide for six reaction solutions of 3.0 mL each plus a small amount to analyze directly by gas chromatography with a flame ionization detection (GC-FID). Catalytic reactions of the model compounds were performed in high pressure mini-autoclave reactors (10 mL total volume) using the general protocol described previously.[10,14] Typically, 50 mg of Cu_{20}PMO and either a 3.0 mL aliquot of pure methanol or a 3.0 mL aliquot of the stock solution were added to the reactors, which were then tightly sealed. For experiments that tracked the mass balance of the solvent, the sealed mini-reactors were weighed using an analytical balance before and after adding the reaction mixture. The reactors were then placed into a pre-heated, custom fabricated, aluminum heating block in a temperature controlled furnace. After the designated reaction time, ranging from 15 min to 18 h, the sample was quenched by rapidly cooling the mini-autoclave in a room temperature water bath or with a high-speed fan (for studies that were concerned with solvent mass balance).

After a catalysis run, the sealed mini-reactors were weighed using an analytical balance after they had cooled to room temperature to ensure that there had been no change in the total mass.

Gas Capture and Analysis. For gas collection from reaction samples, a special apparatus was designed for the volumetric measurement of gases from the mini-autoclave reactors. This device consists of an in-house fabricated aluminum chamber with a vent port, a connecting tube with a sampling port, and a simple water displacement apparatus (SI Figure S1). In the experiments with methanol only, the reactors were resealed and weighed on an analytical balance after venting the gaseous products. Gas composition analysis was performed on an Agilent/HP 6890N (G1530N) gas chromatograph equipped with a thermal conductivity detector (GC-TCD). The GC-TCD instrument was equipped with a 30 m x 0.53 mm fused silica capillary (Supelco carboxen 1010 PLOT) column designed for separating permanent gases and light hydrocarbons. Gas samples (500 100-µL) were injected at a temperature of 225 °C in split mode with a 200:1 ratio and pressure flow control mode at 104.8 kPa, 276 mL/min total flow, 1.4 mL/min column flow, a linear velocity of 32 cm/s and a purge flow of 3.0 mL/min. The temperature program started with a hold at 50 °C for 2 min followed by a 25 °C/min ramp up to 300 °C where the temperature was held for 2 min.

Solution Workup and Analysis. After cooling the reactor and measuring the gas volume and composition, the liquid and solid contents of each individual reaction vessel were separated by pouring the contents into a disposable 10 mL Luer lock syringe equipped with a 0.2-micron filter and a plug of glass wool. The reactor vessel was further washed out with MeOH to give a total volume of 5-6 mL in the disposable syringe. The contents were filtered this way and the liquid portion was used directly for GC-FID analysis and further diluted for gas chromatography-mass spectrometry (GC-MS) analysis.

Compounds were identified by GC-MS using a Shimadzu GC-2010 equipped with a Shimadzu GCMS-QP2010 mass spectrometer detector. On this instrument, 1.0 µL samples were injected at a temperature of 225 °C in split mode with a 200:1 ratio. This GC-MS was equipped with a 30 m x 0.25 mm Agilent DB-1 column with a 0.25 µm lining. The GC program was run in pressure flow control mode at 40 kPa, 162.3 mL/min total flow, 0.79 mL/min column flow, a linear velocity of 32.5 cm/s and a purge flow of 3.0 mL/min. The temperature program started with a hold at 60 °C for 2 min followed by a 25°C/min ramp up to 200 - 300 °C (depending on size and volatility of suspected analytes) where the temperature was held for 4 min. The corresponding MS program had an ion source temperature at 250 °C, interface temperature at 230 °C and recorded from 2.0 to 11.6 min during the GC program.

Quantitative analysis of liquid products was performed on an Agilent/HP 6890N (G1530N) gas chromatograph equipped with a flame ionization detector. This GC-FID instrument was equipped a 30 m x 0.25 mm Agilent DB-1+DG column, with a 0.25 µm dimethylpolysiloxane lining and a guard column. For analysis with this instrument, samples of 0.5-2 µL volume were injected at a temperature of 225 °C in split mode with a 200:1 ratio and pressure flow control mode at 104.8 kPa, 276 mL/min total flow, 1.4 mL/min column flow, a linear velocity of 32 cm/s and a purge flow of 3.0 mL/min. The temperature program

started with a hold at 50 °C or 70 °C for 2 min followed by a 25 °C/min ramp up to 300 °C where the temperature was held for 2 min.

RESULTS AND DISCUSSION

Model Compound Substrates. All studies were carried out using the catalyst Cu_{20}PMO as described above. After a specified reaction time at the specified temperature, a typical run was quenched by rapid cooling. The reactor was then opened and the products analyzed by GC-FID. Products were identified by comparing the retention times to those of known standards and quantified utilizing the effective carbon number (ECN) weighting factor[22,23] to evaluate the GC-FID peak areas relative to the internal standard. Reaction rates were evaluated by global fitting analysis and apparent activation energies (E_a's) were obtained from plots of $\log_e(k_i)$ vs 1/T. (See SI for further details of the analytical methods).[10]

2-Phenoxy-1-phenylethan-1-ol (PPE): PPE is a model for the β-O-4 linkage in lignin. Catalytic disassembly over Cu_{20}PMO was carried out for up to 90 min, with individual time points taken at 15, 30, 45, 60, and 90 min. These sets of reactions were investigated over the temperature range 280-320 °C at 10 degree intervals with the primary goal of determining the apparent E_a value for hydrogenolysis of the β-O-4 linkage. The first products observed were phenol and 1-phenylethanol, the expected HDG products, plus acetophenone, which results from reversible dehydrogenation of 1-phenylethanol owing to the alcohol reforming capabilities of the CuPMO catalyst (Scheme 1). No benzene was found, indicating that HDG of the phenyl-oxygen bond is not significant. At longer reaction times, other secondary products produced by methylation, HDO and/or HYD of these compounds become much more prominent (SI Table S1).

Scheme 1. Primary products for PPE hydrogenolysis over Cu_{20}PMO

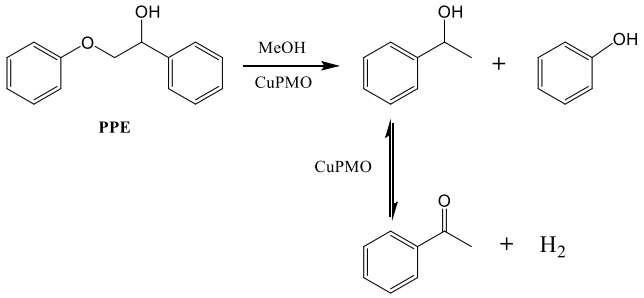

The first notable feature of these experiments is that there was essentially no change in the PPE concentration for the first 15 min, with the exception of the run carried out at 320 °C, where some (<15%) of PPE consumption was observed (Figure 1, SI Table S1). This lag period can be attributed in part to the time needed for these sealed reactors to reach the operating temperature once placed in the oven. Also, as noted below, there is a similar lag in the methanol reforming, so the catalysis may be hydrogen limited during this initial period as well. Kinetics analyses of the primary HDG pathways, as well of secondary reactions, therefore focused on processes occurring after this initial lag period.

At 280 °C, 84% of the PPE was consumed after 1 h (45 min after the 15 min lag period) with phenol, 1-phenylethanol and acetophenone constituting the major products (SI Table S1). According to Scheme 1, the initial products would be one equivalent each of phenol and 1-phenylethanol per PPE consumed. In this context, the phenol product after 1 h reaction at 280 °C represents 93% of that expected based on the consumption of PPE. Cresol, probably formed by methylation of phenol, constitutes another 4% (SI Table S1). In contrast, 1-phenylethanol and acetophenone represent 38% and 32% of the products suggested by Scheme 1 while identified products derived from methylation and HDO of these species make up another 25%. [24]

SI Table S1 summarizes analogous data for PPE experiments carried out at 280, 290, 300, 310 and 320 °C. Global kinetics analysis of the temporal evolution of reactant and products was applied at the different temperatures resulting in calculated first order rate constants for PPE hydrogenolysis (k_{HDG}) under these specific conditions. These fits take into account the observed lag period by starting the analysis at the 15 min time point. Over this temperature range, the apparent values of k_{HDG} for PPE ranged from 1.9 to 7.1 h^{-1}; the differences in individual rate constants as a function of temperature (SI Table S2) being statistically significant. Applying the Arrhenius equation to these temperature dependent rate constants gave an apparent E_a of 83 ± 18 kJ/mol (SI Figure S2). The large experimental uncertainty can be attributed to the corresponding uncertainties in the rate constants owing to the small numbers of data points that can be accumulated in these experiments.

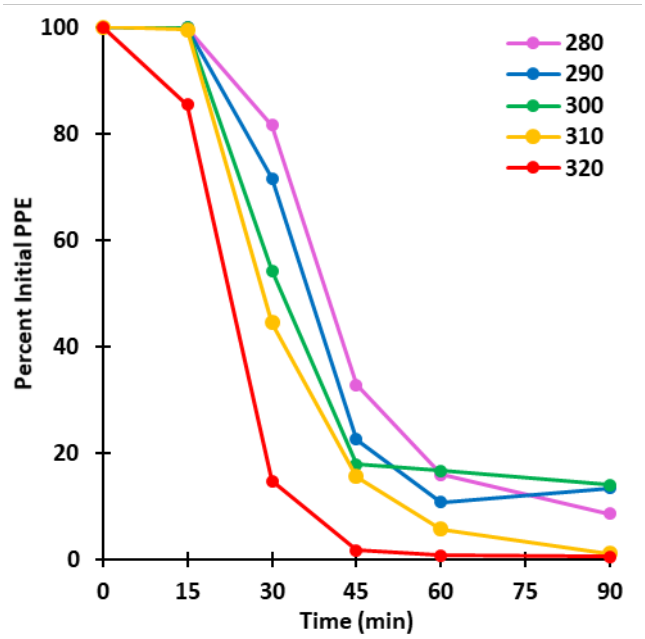

Figure 1. Percent of unreacted PPE found in the reaction mixture at different time-points during 90 min runs over Cu_{20}PMO at temperatures from 280 to 320 °C. Over the first 15 mins there is little discernible change in PPE concentration for each reaction temperatures with the exception of the results for 320 °C, where ~15% depletion of PPE was apparent over this time frame.

Benzyl-phenyl ether (BPE): Catalytic disassembly of BPE, a model for the α-O-4 linkages in lignin, was interrogated over two time courses using the catalyst Cu_{20}PMO in sc-MeOH. Simple HDG of BPE should give (initially) equimolar concentrations of toluene and phenol (Scheme 2). These studies involved preparing a set of identical solutions in separate mini-reactors. For the "long" time course (6 h) reactions, data for individual time points were obtained by quenching a mini-reactor after progressive intervals differing by 1 h each. These studies were run at different temperatures (T) from 280 to 310 °C at 10 degree intervals. An analogous procedure was used for the

"short" time course (120 min) reactions with individual time intervals of 30, 60, 90, and 120 min. For the shorter time course. the reactions were run at 280 to 320 °C at 10 degree intervals.

Scheme 2. HDG of BPE.

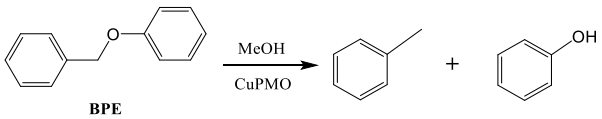

(1)

The 6 h time-course reactions exhibited the product evolution consistent with previous studies under analogous conditions.[10] Initial hydrogenolysis produced toluene in a stoichiometric 1:1 ratio to the BPE consumed (within experimental uncertainty) as predicted by eq. 1. The concurrently formed phenol is considerably more reactive, however, and underwent ring hydrogenation to cyclohexanol or ring methylation to give cresol as well as slower O-methylation to produce anisole, which is relatively unreactive under these conditions.[8,10] The secondary products also underwent successive hydrogenation and/or methylations to give products such as xylenol and methyl-cyclohexanol (Scheme 3).

Given the high reactivity of BPE toward hydrogenolysis, there were but modest differences in BPE conversion at the different temperatures studied. After 1 h, 83% of the benzyl phenyl ether was consumed at 280 °C, while 87% was consumed

Scheme 3. Observed reactions of phenol over Cu_{20}PMO in sc-MeOH

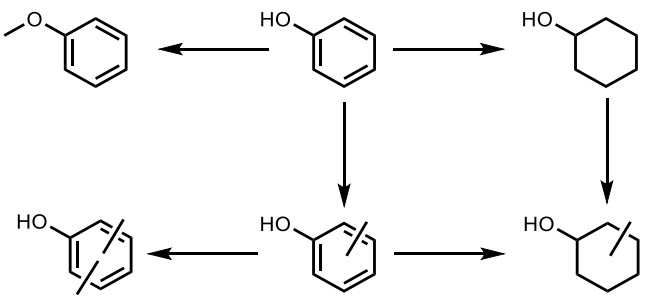

at 290 °C, 91% at 300 °C, and 97% at 310 °C (Figure 2). After 2 h, essentially all of the BPE was consumed in each case. The evolution of the phenol-derived products from subsequent methylation and hydrogenation reactions (SI Table S3) was more sensitive to the reaction conditions. At 2 h, the yield of phenol relative to the BPE consumed at 280, 290, and 310 °C was 82, 68, and 26%, respectively (Figure 2). The 120 min time course experiments followed the pattern seen for the longer ones but provided data relevant to the initial hydrogenolysis of BPE to afford better analysis. (SI Table S4). Global kinetics analysis of BPE consumption gave k_{HDG} values from 1.0 to 4.2 h^{-1} over the temperature range 280 to 320 °C. (SI Table S5). The Arrhenius plot of these k_{HDG} values gave an apparent E_a of 91 ± 8.0 kJ/mol. (SI Figure S3)

Phenol: The reactions of this intermediate of phenol in the hydrogenolysis of BPE and PPE were studied directly under the same conditions. These studies were carried out for 2 h at 280-320 °C (10 degree intervals) with individual time points taken at 30, 60, 90, and 120 min. (SI table S6). The rate constants for phenol hydrogenation k_{HYD}, O-methylation k_{OMe}, and aryl methylation k_{AMe} displayed the ranges 0.023-0.70, 0.022-0.13, and 0.12-0.28 h^{-1}, respectively (SI Table S7). Arrhenius plots gave the respective apparent E_a values 228 ± 30, 108 ± 17, and 61 ± 6 kJ/mol (SI Figure S4).

With regard to the reactivity of the α-O-4 and β-O-4 models BPE and PPE, ether hydrogenolysis displays considerably lower apparent E_a values (83 and 91 kJ/mol, respectively) than does the HYD pathway for phenol (228 kJ/mol).

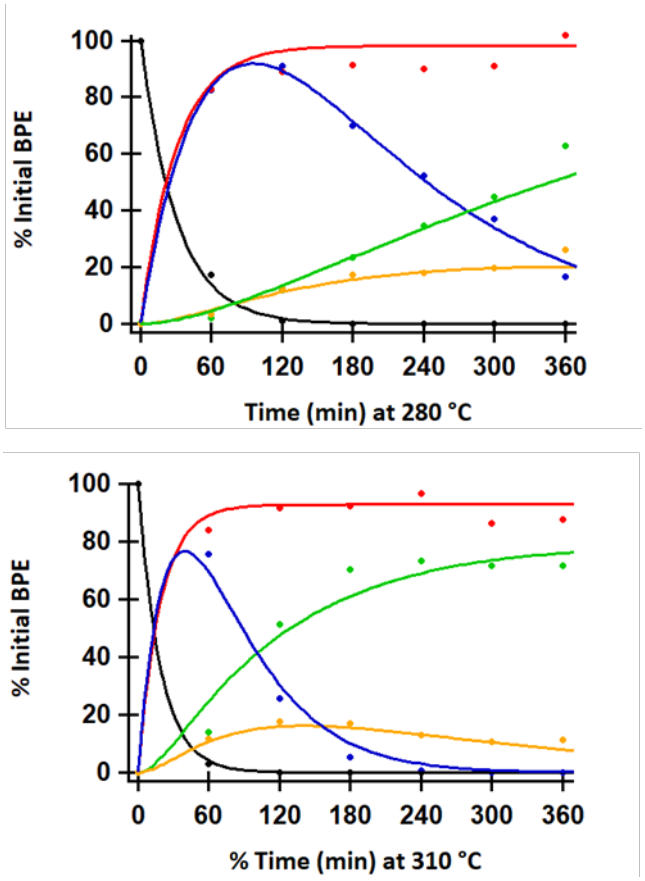

Figure 2. Temporal evolution of BPE (Black), toluene (Red), phenol (Blue) phenol derived aromatics (yellow) and phenol derived aliphatics (green) products during 6 h runs of BPE over Cu_{20}PMO at 280 and at 310 ^{0}C. At both temperatures BPE is completely consumed after 2 h, however there are significantly more aromatics present when T = 280 ^{0}C

Dihydrobenzofuran (DHBF): Catalytic reactions of DHBF (Scheme 4) over Cu_{20}PMO (50 mg) were carried out for up to 18 h, with individual time points taken at 1, 2, 3, 4, 6, 12 and 18 h. This reaction series was run at 290, 300, 320 and 330 °C. The longer time course and higher temperature range compared to BPE and PPE was reflective of the relative recalcitrance of DHBF compared to the other two models.[11] As seen in previous studies, the principal initial product is the ring-opened 2-ethylphenol (EtPhOH) resulting from the hydrogenolysis of the alkyl C-O bond.[14]

At 290 °C only 21% of the DHBF was converted after 6 h, while at higher temperature conversion over this time frame increased significantly with 70% conversion found at 320 °C. It was also possible to track the temperature dependence for the rates of the secondary reactions of the initial EtPhOH product, which underwent HDOto ethylbenzene and HYD to 2-ethylcyclohexanol (SI Tables S8 and S9). Small amounts of ethylcyclohexane were also observed, the apparent result of 2-ethylcyclohexanol HDO.

Arrhenius plots (SI Figure S5) of the calculated rate constants for DHBF hydrogenolysis and subsequent reactions gave

E_a(HDG) = 113 ± 13 kJ/mol and the apparent activation energies for EtPhOH hydrodeoxygenation and hydrogenation E_a(HDO) = 118 ± 11 and E_a(HYD) = 115 ± 12 kJ/mol. However, since EtPhOH hydrogenation is faster than DHBF hydrogenolysis with similar activation energies the slow HDG process is rate limiting at all the temperatures studied.

Scheme 4. Observed initial pathways for DHBF over 50 mg of Cu_{20}PMO in sc-MeOH.

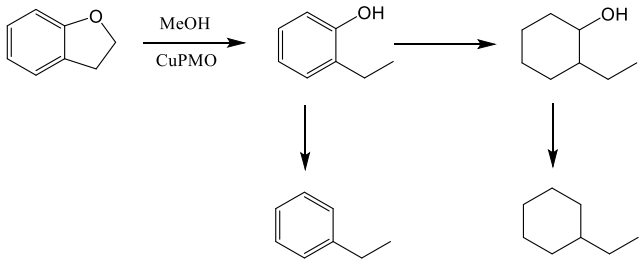

Methanol reforming over Cu_{20}PMO. The hydrogenolysis, hydrodeoxygenation and hydrogenation reactions for the substrates described above all depend on the formation of H_2 via methanol reforming over the Cu_{20}PMO catalyst. Although methanol reformation itself is not rate limiting, this step is critical when considering the tuning of this catalyst since sufficient hydrogen is necessary to prevent char formation. In order to explore this matter further, MeOH reformation by Cu_{20}PMO was studied in the absence of substrate at different temperatures (280 to 320 °C in 10° intervals). In each case, the experiment was initiated with a fixed quantity of freshly calcined catalyst (50 mg) and 3.0 mL of MeOH in 10 mL volume mini-reactors. Individual time points were evaluated from 15 to 195 min at 30 min intervals, and the reaction dynamics were monitored by recording changes in methanol mass and in the volume and composition of the gas produced.

At each temperature studied, there was little or no change in methanol mass during the first 15 min in the reactor. This can be attributed in part to a lag period as the reactors equilibrate to the temperature of the furnace, as seen above with model compounds. Another possible (and not mutually exclusive) explanation for this lag period would be simultaneous transformation of the catalyst to a more active form. Ongoing studies suggest that this is indeed the case, with the first few minutes demonstrating marked structural changes in the catalyst. Since the partial pressure of hydrogen is low at these early stages, it is also likely that a portion of the lag period observed with the model lignin substrates includes the production of enough hydrogen so that it is no longer rate-limiting. After this 15 min lag period, MeOH mass loss was readily apparent, and the rate of such loss increased at the higher temperatures (Figure 3). At the lower temperatures plots of MeOH mass loss versus time were roughly linear consistent with pseudo zero-order kinetics typically observed when a reactant is present in gross excess of a catalyst. However, at higher temperatures, the MeOH mass loss appeared to level out at longer reaction times, suggesting that, in these closed vessel batch reactions, the rate of back reaction, methanol formation, may be approaching that of the reforming process.

The rates of MeOH conversion at each temperature were calculated from the initial slopes of the plots in Figure 3 as 9.3, 12.7, 21.1, 24.2 and 28.6 moles per mole of total Cu in the PMO catalyst per hour at 280, 290, 300, 310 and 320 °C, respectively. These values give an apparent E_a of 79 ± 10 kJ/mol for MeOH consumption.

The gas volumes generated follow a pattern similar to that for methanol consumption, namely a short lag period followed by a relatively linear period of gas production, then a slowing toward an apparent steady state. After reaction for 195 min., the volume of gas released at 295 K and 1.0 atm was 285, 355, 460, 530, and 570 mL for reactions at 280, 290, 300, 310 and 320 °C, respectively. GC-TCD analyses was used to determine the compositions of these gas mixtures.

It is likely that MeOH reforming involves several steps, first dehydrogenation to give formaldehyde and one H_2, followed by conversion of formaldehyde into CO and another H_2. If water is present, such Cu-based catalysts will facilitate the water gas shift ($CO + H_2O == CO_2 + H_2$). A less desirable side reaction would be HDO of MeOH to CH_4 and H_2O, which we have previously reported to be a minor reaction in related systems.[15] Temperature effects on these pathways were evaluated by capturing the gas formed during a batch reaction experiment, measuring the total volume and determining the composition of aliquots by quantitative GC-TCD methods.

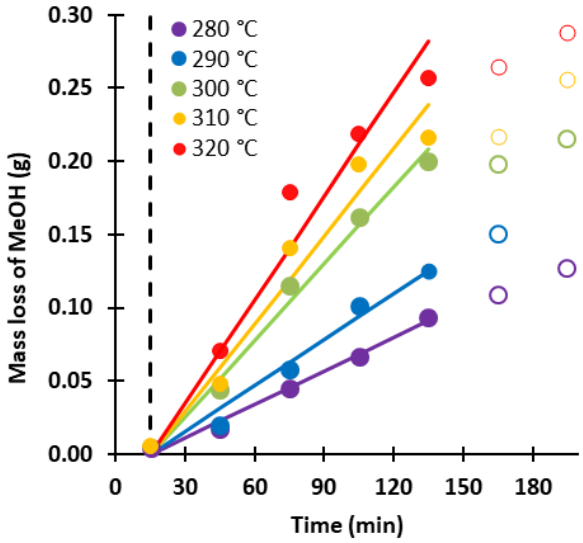

Figure 3. Mass loss of methanol over Cu_{20}PMO (3 mL initial MeOH volume, 50 mg of catalyst) as a function of temperature (280, 290, 300, 310, and 320 °C). Solid markers indicate the time points that were used to calculate the TOF, with the fit lines indicated for each temperature. The open markers indicate time points not used in the fit. The dashed line emphasizes the 15 min time point where only minimal changes in MeOH mass was observed.

Figure 4 illustrates the evolution of the volumes and composition of the gases formed from methanol reforming in a batch reactor operating at 290 °C. The temporal gas volumes and compositions (H_2, CO, CH_4 and CO_2) are summarized in SI Table S10 for each temperature. The gases generated are largely H_2 and CO with the trend in CO production following that of H_2 and the H_2:CO ratio approaching ~2:1 at longer reaction times as expected for the reforming of dry MeOH. Some CO_2 was also found, and this may be largely attributed to the water gas shift owing to the use of reagent CH_3OH that had not been dried rigorously. (Spurious H_2O contamination may be the cause of the anomalous amount of CO_2 generated in the experiment at 310 °C.) Methanol HDO would be another source of water, but

this is clearly a minor side reaction given the small quantities of methane detected (SI Table S10).[25]

Figure 4 also demonstrates the internal consistency between the amount of gas generated and that expected from the mass loss of methanol. The deviance from the expected ratio of hydrogen to the other gases at earlier time points may result from incomplete conversion of formaldehyde to H_2 and CO; however, as noted above, the ratios are more closely linked to those expected later in the time course. Plots similar to Figure 4 for MeOH reforming at each temperature studied are displayed in SI Table S10.

These studies show that production of H_2 via MeOH reforming over CuPMO and the approach to an equilibrium or steady state of the gaseous products occur on a similar time scale as the ether hydrogenolysis of the above models. The first order fits used in interpreting the hydrogenolysis kinetics suggest that, while these tandem processes in the catalytic system are occurring on similar time scales, if sufficient H_2 is present, the HDG rates are not directly dependent on the hydrogen partial pressure P_{H2}. Although P_{H2}increases significantly over a period of several hours, the quantity present even after a relatively short time frame is apparently sufficient to saturate the catalysis sites needed for hydrogenolysis. Furthermore, it is apparent that more hydrogen is produced than necessary for the desired ether hydrogenolysis. The excess H_2 may account for the high rates of phenolic hydrogenation. However, since excess hydrogen is needed in this system to suppress char formation, catalyst modifications or selective poisoning that simply lowers the rate of H_2 production may produce undesirable results. Another approach could be selective poisoning combined with an initial charge of hydrogen to the catalytic system.

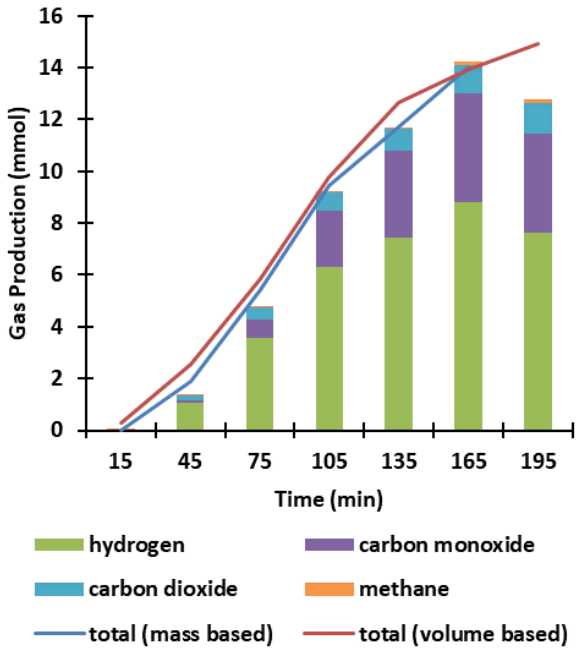

Figure 4: Evolution of gaseous products from the conversion of methanol over Cu_{20}PMO at 290 °C. The stacked bars indicate the mmol of each gas in the total products as determined by GC-TCD. The lines indicate the theoretical total moles of gas based either the total captured volume and ideal gas law (red) or the mass loss of methanol assuming a 3:1 ratio of mol of gas produced per methanol consumed (blue).

SUMMARY

In summary, with regard to the α-O-4 and β-O-4 models BPE and PPE, ether hydrogenolysis displays considerably lower apparent E_a values than does the HYD pathway for the initial phenol product. On the other hand, DHBF ether hydrogenolysis has a comparable Ea at 113 kJ/mol but the individual rates were among the slowest observed in this study. The overall similarity of the observed E_a's for ether hydrogenolysis suggests a similar mechanism for these substrates, with the differences in overall rates and the trend in E_a matching the relative ether bond strengths in the individual model compounds.[26]

These studies demonstrate that lower operating temperatures and limited contact time can improve the selectivity towards aromatic products. At least from these batch reactor systems with model compounds, it is clear that one can enhance the aromatic composition of product streams by controlling reaction temperature. For example, at 290 °C the α-O-4 and the β-O-4 ether linkages in the models are largely cleaved by hydrogenolysis after 90 min, while there was relatively little hydrogenation and other secondary reactions of the initial aromatic products. However, although with genuine lignin, the β-O-4 and α-O-4 linkages between the mono-lignol fragments are the most common, there are other more recalcitrant linkages that would ensure that the products generated will be a mixture of monomers and small oligomers requiring additional processing.[11]

With regard to the reformation of methanol to produce reducing equivalents of H_2, these studies demonstrate an observed E_a for the conversion of methanol of ~80 kJ/mol. It was also observed that the continued production of H_2 during the first three hours did not affect the first order model for ether hydrogenolysis, suggesting that a sufficient concentration of H_2 is produced during the initial stages of the disassembly reactions to saturate the active sites in the catalyst. While a high rate of H_2 production is desirable to reduce char formation, it is likely that H_2 is overproduced in the batch reactions described in this study.

Notably, these studies clearly show that the distribution of products is dependent on the contact time with the catalyst. Combined with the potential for temperature and P_{H2} control, this points to the likely advantage of utilizing flow reactors to control the product distributions in the future.

ASSOCIATED CONTENT

Supporting Information

The Supporting Information is available free of charge on the ACS Publications website.

Expanded descriptions for sample preparation, experimental workup, and analysis of catalyzed reactions. 5 figures and 10 tables (PDF)

AUTHOR INFORMATION

Corresponding Author

* Peter C. Ford: ford@chem.ucsb.edu

Author Contributions

All authors have given approval to the final version of the manuscript.

Notes

The authors declare no competing financial interest.

ACKNOWLEDGMENT

These studies were largely supported by the Center for the Sustainable Use of Renewable Feedstocks (CenSURF), a NSF Center for Chemical Innovation (NSF CHE-1240194). HM acknowledges funding from the Thailand Research Fund through a Royal Golden Jubilee Scholarship (Grant No. PHD/0013/2554), the Ratchadapisake Sompote Endowment Fund, and the Center of Excellence for Petrochemical and Materials Technology, Chulalongkorn University, Thailand, while MB acknowledges funding from the Sao Paulo Research Foundation, Brazil (FAPESP 2012/10884-0).

REFERENCES

(1) Ragauskas, A.J.; Beckham, G. T.; Biddy, M. J.; Chandra, R.; Chen, F.; Davis, M.F.; Davison, B.H.; Dixon, R. A.; Gilna, P.; Keller, M.; Langan, P.; Naskar, A. K.; Saddler, J. N.; Tschaplinski, T. J.; Tuskan, G. A.; Wyman, C. E. Lignin valorization: improving lignin processing in the biorefinery. *Science* **2014**, *344*, 1246843.

(2) Zakzeski, J.; Bruijnincx, P. C. A.; Jongerius A. L.; Weckhuysen, B. M. The catalytic valorization of lignin for the production of renewable chemicals. *Chem. Rev.* **2010**, *110*, 3552–3599.

(3) Ragauskas, A. J.; Williams, C. K.; Davison, B. H.; Britovsek, G.; Cairney, J.; Eckert, C. A.; Frederick Jr., W. J.; Hallett, J. P.; Leak, D.J.; Liotta, C. L.; Mielenz, J. R.; Murphy, R.; Templer, R.; Tschaplinski, T. The path forward for biofuels and biomaterials *Science* **2006**, *311*, 484−489.

(4) Boerjan, W.; Ralph, J.; Baucher, M. Lignin Biosynthesis, *Annu. Rev. Plant Biol.*, **2003**, *54*, 519–546.

(5) Sannigrahi, P.; Ragauskas, A. J.; Tuskan, G. A. Poplar as a feedstock for biofuels: A review of compositional characteristics. *Biofuels, Bioprod. Biorefin*. **2010**, *4*, 209−226.

(6) Froass, P. M.; Ragauskas, A. J.; Jiang, J. Chemical Structure of Residual Lignin from Kraft Pulp. *J. Wood Chem. Technol.* **1996**, *16*, 347−365.

(7) Barta, K.; Warner, G. R.; Beach, E. S.; Anastas, P. Depolymerization of organosolv lignin to aromatic compounds over Cu-doped porous metal oxides. *Green Chem.* **2014**, *16*, 191-196.

(8) Barrett, J. A.; Gao, Y.; Bernt, C. M.; Chui, M.; Tran, A. T.; Foston, M. B.; Ford, P. C. Enhancing aromatic production from reductive lignin disassembly: in situ O-methylation of phenolic intermediates. *ACS Sustainable Chem. Eng.* **2016**, *4*, 6877-6886.

(9) Barta, K.; Ford, P. C. Catalytic conversion of nonfood woody biomass solids to organic liquids *Acc. Chem. Res.* **2014**, *47*, 1503-1512.

(10) Bernt, C. M.; Bottari, G.; Barrett, J. A.; Scott, S. L.; Barta, K.; Ford, P. C. Mapping reactivities of aromatic models with a lignin disassembly catalyst. Steps toward controlling product selectivity. *Catal. Sci. Tech.* **2016**, *6*, 2984-2994.

(11) Chui, M.; Metzker, G.; Bernt, C. M.; Tran, A. T.; Burtoloso, A. C.; Ford, P. C. Probing the lignin disassembly pathways with modified catalysts based on Cu-doped porous metal oxides. *ACS Sustainable Chem. Eng.* **2017**, *5*, 3158-3169.

(12) Huang, Y.-B.; Yan, L.; Chen, M.-Y.; Guo, Q.-X.; Fu, Y. Selective Hydrogenolysis of Phenols and Phenyl Ethers to Arenes through Direct C-O Cleavage over Ruthenium-Tungsten Bifunctional Catalysts. *Green Chem.* **2015**, *17*, 3010-3017.

(13) Molinari, V.; Giordano, C.; Antonietti, M.; Esposito, D. Titanium Nitride-Nickel Nanocomposite as Heterogenous Catalyst for the Hydrogenolysis of Aryl Ethers. *J. Am. Chem. Soc.* **2014,** *136*, 1758-1761.

(14) Hanson, S. K.; Baker, R. T. Knocking on Wood: Base Metal Complexes as Catalysts for Selective Oxidation of Lignin Models and Extracts. *Accts. Chem. Res*. **2015**, *48*, 2037-2048.

(15) Luo, N.C.; Wang, M.; Li, H.; Zhang, J.; Hou, T.; Chen, H.; Zhang, X. C.; Lu, J.; Wang. F. Visible-Light-Driven Self-Hydrogen Transfer Hydrogenolysis of Lignin Models and Extracts into Phenolic Products, *ACS Catal.* **2017**, *7*, 4571-4580

(16) Macala, G. S.; Matson, T. D.; Johnson, C. L.; Lewis, R. S.; Iretskii, A. V.; Ford, P. C. Hydrogen Transfer from Supercritical Methanol over a Solid Base Catalyst: A Model for Lignin Depolymerization. *Chem. Sus. Chem.* **2009**, *2*, 215-217.

(17) Matson, T. D.; Barta, K.; Iretskii, A. V.; Ford, P. C. One-pot catalytic conversion of cellulose and of woody biomass solids to liquid fuels. *J. Am. Chem. Soc.* **2011**, *133*, 14090−14097.

(18) Huang, X.; Korányi, T. L.; Boot, M. D.; Hensen, E. J. M. Catalytic Depolymerization of Lignin in Supercritical Ethanol *Chem. Sus. Chem.* **2014**, *7*, 2276-2288.

(19) Luo, H.; Klein, I. M.; Jiang, Y.; Zhu, H.; Liu, B.; Kenttamaa, H. L.; Abu-Omar, M. M. Total utilization of miscanthus biomass, lignin and carbohydrates, using earth abundant nickel catalyst. *ACS Susatinable Chem. Eng.* **2016**, *4*, 2316-2322.

(20) Nichols, J. M.; Bishop, L. M.; Bergman, R. G.; Ellman, J. A. Catalytic Bond Cleavage of 2-Aryloxy-1-arylethanols and Its Application to the Depolymerization of Lignin-Related Polymers. *J. Am. Chem. Soc.* **2010**, *132*, 12554-12555.

(21) Cosimo, J. I.; Diez, V. K.; Xu, M.; Iglesia, E.; Apesteguia, C. R. Structure and Surface and Catalytic Properties of Mg-Al Basic Oxides. *J. Catal.* **1998**, *178*, 499-510.

(22) Sternberg, J.C.; Gallaway, W.S.; Jones, D.T.L. The mechanism of response of flame ionization detectors. In ***Gas Chromatography.*** N. Brenner, J.E. Callen, and M.D. Weiss, eds. Academic Press, New York, **1962**, pp. 231-67.

(23) Scanlon, J. T.; Willis, D. E. Calculation of Flame Ionization Detector Relative Response Factors Using the Effective Carbon Number Concept. *J. Chromatogr. Sci.* **1985**, *23*, 333-340.

(24) A referee has suggested an alternate pathway for this substrate where dehydrogenation of the alcohol function would first give 2-phenoxy-1-phenylethanone followed by hydrogenolysis of the ether function to give acetophenone and phenol. Although the 2-phenoxy-1-phenylethanone intermediate was not observed, the formation of acetophenone as a significant product would be consistent with such a pathway. Regardless of the sequence of steps, it is notable 2-phenoxy-1-phenylethanol is a more reactive substrate under these conditions than is the 2-phenoxy-1-phenylethane studied in this laboratory previously,[11] so the additional hydroxyl group does play a significant role in promoting disassembly of these aromatic ethers.

(25) A reviewer has suggested that dimethyl ether (DME) might also be expected as a product of Lewis acid catalysis by the CuPMO catalysts and that this might be an additional source of H_2O. Given the very low boiling point of DME (–24 ^oC), we would have expected to have easily detected this product in the GC analyses, but did not. DME was, however, detected in earlier studies by this laboratory during longer time scale reactions (8h).[17] This implies that either DME is a very minor product under the present conditions or its presence is masked by the overlap with other peaks in the GC-FID and GC-TCD methods, or possibly it is not stable under these conditions.

(26) Seonah, K.; Chmely, S. C.; Nimlos, M. R.; Bomble, Y. J.; Foust, T. D.; Paton, R. S.; Beckham, G T.; Computational Study of Bond Dissociation Enthalpies for a Large Range of Native and Modified Lignins. *J. Phys. Chem. Lett.* **2011**, *2*, 2846-2852.

For Table of Contents Use Only:

Temperature tuning of product evolution from lignin model reactions with Cu-doped PMO catalysts in sc-MeOH promises more selectivity in biomass conversion to chemicals and fuels.